



HAL
open science

RADIOLYTIC CORROSION OF GRAIN BOUNDARIES ONTO THE UO₂ TRISO PARTICLE SURFACE

A. Traboulsi, Johan Vandendorre, G. Blain, J. Barbet, M. Fattahi

► **To cite this version:**

A. Traboulsi, Johan Vandendorre, G. Blain, J. Barbet, M. Fattahi. RADIOLYTIC CORROSION OF GRAIN BOUNDARIES ONTO THE UO₂ TRISO PARTICLE SURFACE. 7th EC FP CP FIRST-Nuclides 1st Annual Workshop 2012, Oct 2012, Budapest, Hungary. in2p3-00911332

HAL Id: in2p3-00911332

<https://in2p3.hal.science/in2p3-00911332v1>

Submitted on 29 Nov 2013

HAL is a multi-disciplinary open access archive for the deposit and dissemination of scientific research documents, whether they are published or not. The documents may come from teaching and research institutions in France or abroad, or from public or private research centers.

L'archive ouverte pluridisciplinaire **HAL**, est destinée au dépôt et à la diffusion de documents scientifiques de niveau recherche, publiés ou non, émanant des établissements d'enseignement et de recherche français ou étrangers, des laboratoires publics ou privés.

RADIOLYTIC CORROSION OF GRAIN BOUNDARIES ONTO THE UO₂ TRISO PARTICLE SURFACE

Johan Vandendorre^{1*}, Ali Traboulsi¹, Guillaume Blain¹, Jacques Barbet², Massoud Fattahi¹

¹ SUBATECH, Unité Mixte de Recherche 6457, Ecole des Mines de Nantes, CNRS/IN2P3, Université de Nantes, 4 rue Alfred Kastler, BP 20722, 44307 Nantes cedex 03, France.

² Cyclotron ARRONAX, 1 Rue ARRONAX, 44817 St-Herblain Cedex France

* Corresponding author: johan.vandendorre@subatech.in2p3.fr.

Abstract

This work is dealing with the understanding of the corrosion mechanisms at solid/solution interface and taking into account for the $^4\text{He}^{2+}$ ions irradiation effects on these mechanisms. These corrosion and $^4\text{He}^{2+}$ ions radiolysis phenomena append at solid/solution interface and will be studied at a μmetric scale by the Raman spectroscopy. Moreover, a $^4\text{He}^{2+}$ ions irradiation appends onto a low volume and let us to control the irradiated area (solution, solid or interface). For the solid, the chemical species induced by $^4\text{He}^{2+}$ ions radiolysis of water are such reactive and are involved in classical corrosion mechanisms of UO_2 . Moreover, we want to study the impact of the $^4\text{He}^{2+}$ ions radiolysis of water layers physisorbed into the surface onto corrosion mechanisms. That is the reason why we want to use a local irradiation, allowed by the $^4\text{He}^{2+}$ ions ion beam provided by the ARRONAX cyclotron ($E = 64.7 \text{ MeV}$). In this work an experimental apparatus will be performed in order to characterize solid/solution interface at μmetric scale by Raman spectroscopy under $^4\text{He}^{2+}$ ions irradiation provided by the cyclotron ARRONAX facility. The leaching experiments under irradiation will be performed for a short time in order to study the parameters during the fast instant release step. The grain boundaries effect will be studied by the comparison between one TRISO particles set (solids with grain boundaries) and one TRISO particles set previously washed by one acid solution (solid without grain boundaries). The role of H_2 will be studied by the comparison between experiments under Ar or Ar/ H_2 atmosphere. The dose rate range will be between 0 and 100 Gy/min by using the alpha ion beam which let us control the dose set down into the sample. For all these experiments, measurements will be performed by the *in situ* Raman spectroscopy during the irradiation in order to follow the formation/consumption of the secondary phases formed onto the solid. The SEM will be performed in order to characterize the grain boundaries and the secondary phases formed by the leaching/irradiation experiments. The μGC is used to measure the P_{H_2} into the irradiation cell to follow the production/consumption of this gaseous species formed by the water radiolysis and consumed by the leaching process.

Introduction

This paper deals with the radiolytic corrosion at the UO₂ surface. We study the impact of the water radiolysis onto the corrosion of the grain boundaries (GB) detected at the TRISO particle surface. Moreover, the H₂ influence onto the corrosion is studied. In more details, the conditions of these experiments are described below:

- UO₂ TRISO particle natural: This work deals with the impact of the GB present at the UO₂ TRISO particle surface. We want to study the effect of the GB onto the dissolution (It has been ever shown that for ThO₂ TRISO particle it is the GB which control the solubility (Vandenborre et al., 2010)). Moreover, information provided onto the GB impact onto the UO₂ TRISO particle dissolution can be relevant for the instant release fraction because IRF is linked to the GB phase onto the Spent Fuel surface.
- Pure water irradiated: We want to study the effect of the radiolysis, classically induced by the high burn-up spent UO₂ fuel, by an external alpha beam with a large scale of dose rate (between 0 and 100 Gy/min) in order to study the radiolytic dissolution of UO₂ and its secondary phases. Moreover, the dose rate of about 25 Gy/min corresponds to the dose rate delivered by the high burn-up spent UO₂ fuel (Grambow et al., 2010). Then, we study the solid surface dissolution by the water radiolysis coming not from the high burn-up spent UO₂ fuel but by a controlled alpha beam. This alpha beam is controlled for the dose rate, the localisation of the 30 μm layer irradiated (in water, onto the surface, into the GB...) in order to determine the impact of this localisation onto the IRF. Moreover, the water radiolysis produces molecular species such as H₂O₂ which play a non negligible role into the UO₂ corrosion mechanism as described in the literature (Corbel et al., 2001; Ekeroth et al., 2006; Jégou et al., 2005; Jonsson et al., 2004; Roth and Jonsson, 2008; Suzuki et al., 2006).
- H₂ effect: is studied (induced by the water radiolysis or initially merged in the system) onto the dissolution of the GB. In fact, we are able to measure the H₂ produced or consumed by the radiolysis/dissolution mechanisms and to bring information onto the reactivity of the IRF vs. the H₂, in particular at 0.02 M (=0.16 bar) corresponding to experimental conditions performed in previous European Projects (MICADO, SFS). Moreover, the H₂ quantity implied during the dissolution of GB phases can be measured.
- UO₂ secondary phases characterization and evolution can be followed by the *in situ* Raman spectroscopy. The kinetic (from a few minutes to a few days) of formation/consumption of the secondary phases onto the UO₂ surface (with a localization at the GB by μ-Raman technique) give data onto the formation/consumption of the instant release fractions. Raman experiments have been successfully performed onto the UO₂ surface with good results for the determination of schoepite and studite phases at the UO₂ surface as described in the literature (Amme et al., 2002; Biwer et al., 1990; Carbol et al., 2005; Corbel et al., 2006; Eary and Cathles, 1983; Hanson et al., 2005; He and Shoemith, 2010; Sattonnay et al., 2001).

Also, this work can answer to the GB formation, depletion, evolution, reactivity vs. alpha external dose rate, [H₂] at the UO₂ surface for the FIRST-NUCLIDES Project. Moreover, it seems relevant for the retention process to know the secondary phases formation/depletion by the radiolytic chemical reactions and the effect of H₂ onto these phases.

Material and Methods

Samples

UO₂ TRISO particles are purchased by Pr. Fachinger from FZJ. Synthesis detailed into (Brähler et al., 2012) with, in particular, a calcination step which was performed at 1600°C for UO₂ crystallization. Physico-mechanical Characterization and first solubility tests were ever performed in the literature (Bros et al., 2006; Grambow et al., 2008; Titov et al., 2004). Solid analysis is performed by SEM (scanning electron microscopy, JEOL 5800 SV with a 15 kV voltage) and the SEM samples were covered by a Pt layer in order to improve electron conduction and increase the picture resolution. Mechanical separation of C-layers from the UO₂ spheres is performed in order to analyse the sphere (**Figure 2**). **Table 1** shows the properties of the UO₂ spheres after the separation step. Moreover, we have checked by EDX that the chemical composition of the sphere surface is only UO₂.

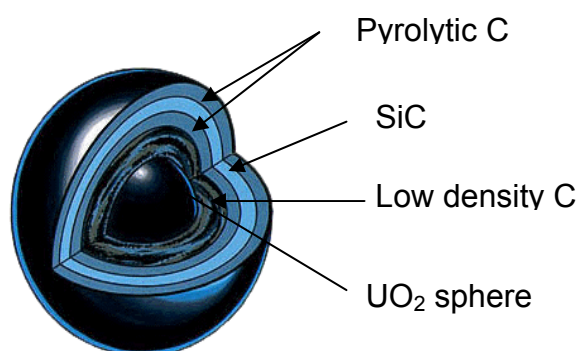


Figure 1: UO₂ spheres with different C-layers from (Brähler et al., 2012).

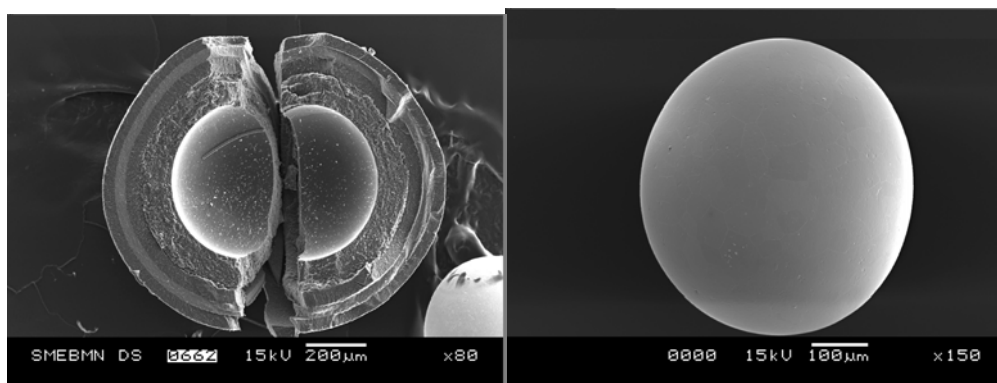


Figure 2: SEM picture of UO₂ TRISO particle after the separation step, Left: C-Layers, Right: UO₂ sphere

Table 1: Properties determined for the UO₂ sphere.

Sphere	UO ₂ (cr)
Diameter (mm)	0.50
Weight (mg)	0.76
Density (g.cm ⁻³)	10.96
Geometric Surface Area (m ² .g ⁻¹)	1.05 10 ⁻³

The pre-washing batch experiments were performed exposing unirradiated UO₂ TRISO particles to an aqueous solution in undersaturated conditions. A HDPE (High Density polyethylene) reaction vessel is used, containing 15 ml of a 0.1 mol.L⁻¹ HCl solution under continuous stirring during 15 days in order to deplete the GB phases.

Irradiation experiments

⁴He²⁺ ions irradiations are provided by the ARRONAX cyclotron facility (Saint-Herblain, France) onto a vertical beam-line. Experiments are carried out within ARRONAX cyclotron at 64.7 MeV. The intensity of the particles beam, measured on an internal Faraday cup located one meter upstream, is maintained at 70 nA. The uncertainty of that current measurement is of 10 %. Fricke dosimetry (Fricke and Hart, 1966) is used in this study in order to determine the dose deposited into the samples. This method is based on the oxidation of Fe²⁺ to Fe³⁺ by the species produced by the water radiolysis reactions. The concentration of ferric ions is monitored by UV-Vis measurements at 304 nm ($\epsilon = 2197 \text{ L.mol}^{-1}.\text{cm}^{-1}$, 298 K) with a spectrophotometer CARY4000 (VARIAN). These measurements are carried out on samplings few minutes after irradiation. Super Fricke solutions are prepared by dissolving the desired quantity of Mohr's salt ($[\text{Fe}^{2+}] = 10 \text{ mmol.L}^{-1}$) and NaCl (1 mmol.L⁻¹) in aerated aqueous 0.4 mol.L⁻¹ H₂SO₄ solutions. All reagents are analytical grade or equivalent. NaCl is added in order to avoid any organic impurities. The irradiation time is a few minutes for ARRONAX experiments. The dose rates were measured at 7500 Gy.min⁻¹ during irradiation in the ARRONAX facility using the ferric ion radiolytic yield extrapolated from the literature (LaVerne and Schuler, 1987; Matsui et al., 1970; Saini and Bhattacharyya, 1987) ($G(\text{Fe}^{3+}) = 5.0 \cdot 10^{-7} \text{ mol.J}^{-1}$ for $E = 5.0 \text{ MeV}$ and $G(\text{Fe}^{3+}) = 11.7 \cdot 10^{-7} \text{ mol.J}^{-1}$ for $E = 64.7 \text{ MeV}$).

At the ARRONAX cyclotron, 2 mL of solution is introduced into the irradiation cell. Due to the small penetration depth of ⁴He²⁺ ions in water, the volumic irradiated fraction is small.

In situ Raman experiments

All the Raman system is purchased by the HORIBA Jobin-Yvon Company. Raman spectra are recorded with an iHR550 spectrometer equipped with two optic fibers (diameter = 100 μm , length = 20 m). The detector is a charged coupled device (CCD) cooled by Peltier effect (203 K). Raman spectra are excited with a laser beam at 632.8 nm emitted by a He/Ne Laser. The laser beam is weakly focused on samples with a diameter of about 1 mm and a power of about 14 mW for a working distance of 40 mm on the sample and an acquisition time of 2 minutes. The Raman backscattering is collected through an objective system and dispersed by 1200 grooves/mm gratings to obtain 5 cm⁻¹ spectral resolution for Raman stokes spectra excited at 632.8 nm. The wavenumber accuracy was checked and considered better than 0.5 cm⁻¹.

With the Raman spectroscopic device (laser excitation and back scattering Raman) described before, *in situ* experiments have been performed onto the solid samples in contact with ultrapure water. **Figure 3** displays the device installed onto the ⁴He²⁺ beam line. The ⁴He²⁺ ions beam is provided by the ARRONAX cyclotron facility with $E = 64.7 \text{ MeV}$. The average

length of the ${}^4\text{He}^{2+}$ particle for this energy is determined at about 2.5 mm in the ultrapure water solution by the SRIM 2008 simulation code (Ziegler et al., 1985; Ziegler et al., 2010). Thus, we could have checked experimentally that for a volume solution of 2 mL, with a solid/ ${}^4\text{He}^{2+}$ -beam distance of 5 mm, the ${}^4\text{He}^{2+}$ ions irradiation direct effects occur onto the solution and not onto the solid surface. So, with this *in situ* experimental device experiment under irradiation, this work can be devoted to study the effect of the water radiolysis species onto the solid corrosion and the direct irradiation consequences onto the solid surface.

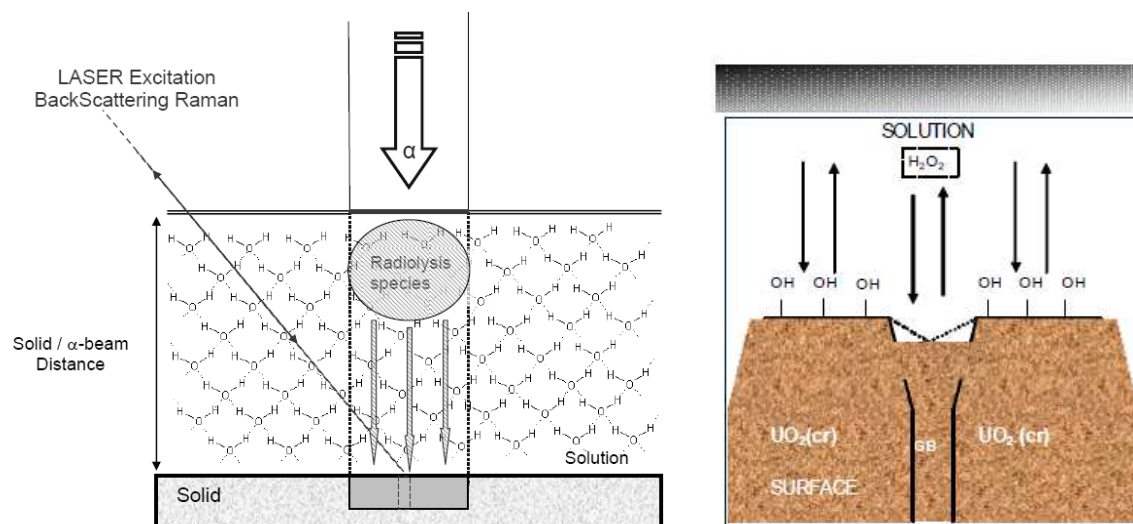


Figure 3: Left: *In situ* Raman spectroscopic device experiment under ${}^4\text{He}^{2+}$ ions beam irradiation onto the ARRONAX facility vertical beam line, Right: Zoom at the UO_2 TRISO particle surface with $\text{UO}_2(\text{cr})$ and GB phases

Results

1. WPI Results

1.1 Irradiation cell development

First test experiments of *in situ* Raman analysis have been performed with a first version of our irradiation cell which let us to analyze the surface with Raman spectroscopy (See **Figure 4**). However, we are developing a new version in order to analyze respectively, during the alpha irradiation, the solid by the Raman spectroscopy and the solution by the UV-VIS spectrophotometry. Moreover, with the cell we will be able to measure the Hydrogen into the system by $\mu\text{-GC}$ (See **Figure 5**). This complete analytic system will be useful in order to determine the Uranium speciation at the surface, in the solution during the irradiation and to measure the Hydrogen produced or consumed by the chemical system.

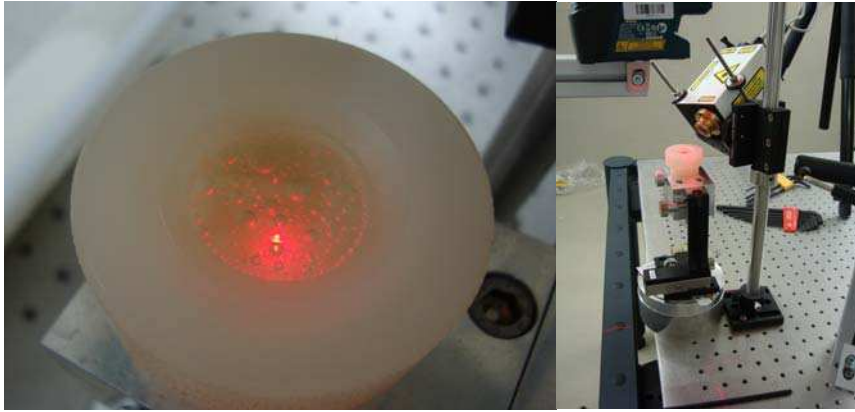


Figure 4: Left: Irradiation cell with H_2 bubbles produced by the water radiolysis, Right: In situ Raman spectroscopic device experiment under $^4He^{2+}$ ions beam irradiation onto the ARRONAX facility vertical beam line



Figure 5: Left: New measurement cell with UV-VIS probe, Right: Schematic picture of the new In situ Raman spectroscopic cell

1.2 SEM pictures

A pre-washing experiment has been performed in order to study UO_2 TRISO particle with and without GB. By this way, we will determine the impact of the GB onto the radiolytic dissolution process of the UO_2 TRISO particle. First SEM pictures analysis were performed onto two samples. The UO_2 TRISO particle surfaces were analyzed before and after the pre-washing step (Respectively **Figure 6** and **Figure 7**).

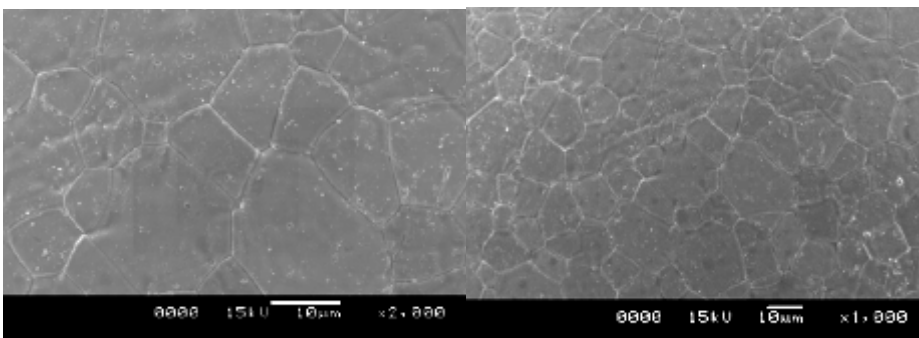


Figure 6: SEM pictures of the UO_2 TRISO particle BEFORE the pre-washing step

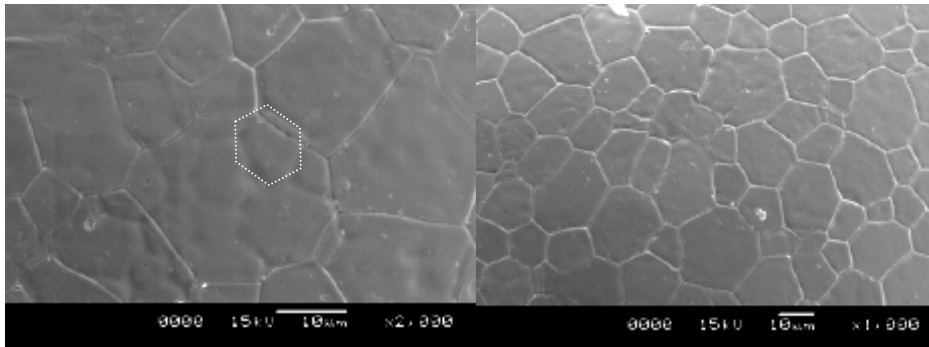


Figure 7: SEM pictures of the UO₂ TRISO particle AFTER the pre-washing step

From these pictures, the grain size average can be determined about $15 \pm 5 \mu\text{m}$. Moreover, the pre-washing process involves a dissolution of the C-layers remained at the UO₂ surface. Moreover, new grains, with GB too, occur at the UO₂ surface with a lower grain size average. The next step of this work is to analyze, by μ -Raman spectroscopy, the surface with UO₂(cr) grain and GB(I), from the solid sintering, and GB(II), from the pre-washing process.

2. WP2 Results

The spectra of the first tests of *in situ* Raman experiment under alpha irradiation were shown in **Figure 8**. The spectra have been monitored versus the irradiation time (1 to 6 min). We can recognize the typical fundamental UO stretch Raman band at 443 cm^{-1} of the UO₂. Nevertheless, the sensitivity is too low in order to determine the evolution of the Raman spectra versus the irradiation time. So, we are not yet able to detect accurately the UO₂ secondary phases such as schoepite or studite in the Raman spectra are at $800\text{-}870 \text{ cm}^{-1}$ (Amme et al., 2002; Aubriet et al., 2006; Biwer et al., 1990; Hoekstra and Siegel, 1973; Sobry, 1973). That is the reason why, in the next step of this task, we will install a new powerful LASER with a higher excitation wavelength of 532 nm in order to increase the sensitivity of our experimental device.

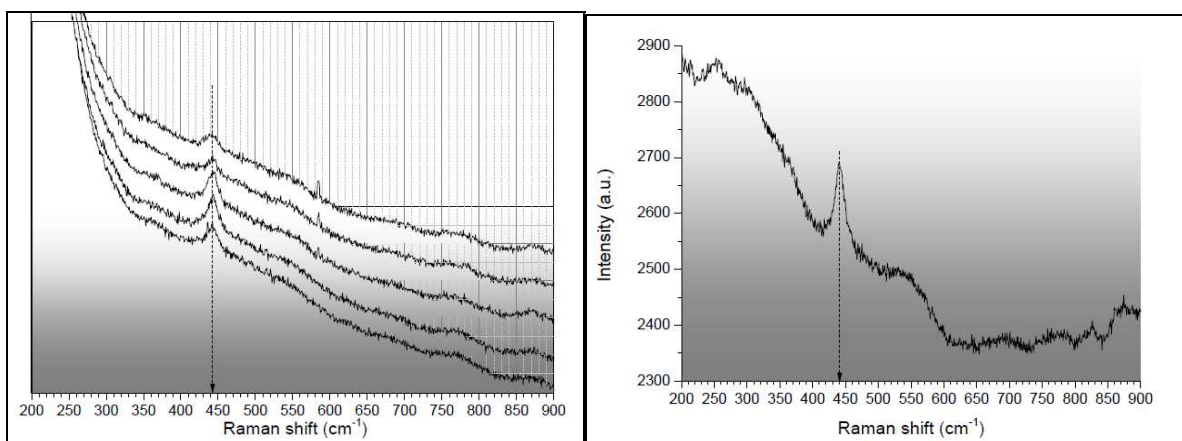


Figure 8: Raman spectra of the UO₂ TRISO particle, Left: For irradiation times from 1 to 5 min, Right: For irradiation time of 6 min

Conclusions and Future work

The future works planned for this task:

- A complete Uranium speciation during the radiolytic corrosion respectively into the solution by UV-VIS Spectrophotometry and at the solid surface by Raman analysis.
- Improvement of the Raman detection in order to increase the sensitivity by a green excitation LASER (532 nm), a higher time resolution for the mechanisms kinetics determination at a higher spatial scale for the discrimination between the UO₂(cr) grain and the GB analysis.
- A Hydrogen impact study onto the radiolytic corrosion by the control and the measurement of the atmosphere in the irradiation cell in order to determine the part of H₂ which occurs into the radiolytic corrosion process.
- Finally, after the FIRST-NUCLIDES Project in a few years, the same system will be used into an Irradiated TRISO particle in order to study a more realistic system close to the Spent Nuclear Fuel. Then, this work is the first step of the complete study.

Acknowledgement

We acknowledge B.Humbert and J.Y. Mevellec from the IMN laboratory for support in Raman measurements and N.Stephant for SEM measurements. The authors acknowledge ARRONAX staff for the efficient performing of irradiation runs onto the cyclotron facility.

The research leading to these results has received funding from the European Union's European Atomic Energy Community's (Euratom) Seventh Framework Programme FP7/2007-2011 under grant agreement n° 295722 (FIRST-Nuclides project).

References

Amme, M., Renker, B., Schmid, B., Feth, M.P., Bertagnolli, H., Döbelin, W., 2002. Raman microspectrometric identification of corrosion products formed on UO₂ nuclear fuel during leaching experiments. *Journal of Nuclear Materials* 306, 202-212.

Aubriet, H., Humbert, B., Perdicakis, M., 2006. Interaction of U(VI) with pyrite galena and their mixtures a theoretical and multitechnique approach *Radiochimica Acta* 94, 657-663.

Biwer, B.M., Ebert, W.L., Bates, J.K., 1990. The Raman spectra of several uranyl-containing minerals using a microprobe. *Journal of Nuclear Materials* 175, 188-193.

Brähler, G., Hartung, M., Fachinger, J., Grosse, K.-H., Seemann, R., 2012. Improvements in the fabrication of HTR fuel elements. *Nuclear Engineering and Design*.

Bros, P., Mouliney, M.H., Millington, D., Sneyers, A., Fachinger, J., Vervondern, K., Roudil, D., Cellier, F., Abram, T.J., 2006. Raphael project- HTR specific waste characterization programme. *Proceedings HTR2006 : 3rd International Topical Meeting on High Temperature Reactor Technology* B00000162.

Carbol, P., Cobos-Sabate, J., Glatz, J.P., Ronchi, C., Rondinella, V., Wegen, D.H., Wiss, T., Loida, A., Metz, V., Kienzler, B., Spahiu, K., Grambow, B., Quinones, J., Martinez Esparza Valiente, A., 2005. The effect of dissolved hydrogen on the dissolution of ²³³U doped UO₂(s), high burn-up spent fuel and MOX fuel, in: Co, S.N.F.a.W.M. (Ed.), Report. SFS EU-Project, Stockholm.

Corbel, C., Sattonnay, G., Guilbert, S., Garrido, F., Barthe, M.F., Jegou, C., 2006. Addition versus radiolytic production effects of hydrogen peroxide on aqueous corrosion of UO₂. *Journal of Nuclear Materials* 348, 1-17.

Corbel, C., Sattonnay, G., Lucchini, J.-F., Ardois, C., Barthe, M.-F., Huet, F., Dehaut, P., Hickel, B., Jegou, C., 2001. Increase of the uranium release at an UO₂/H₂O interface under He²⁺ ion beam irradiation. *Nuclear Instruments and Methods in Physics Research Section B: Beam Interactions with Materials and Atoms* 179, 225-229.

Eary, L., Cathles, L., 1983. A kinetic model of UO₂ dissolution in acid, H₂O₂ solutions that includes uranium peroxide hydrate precipitation. *Metallurgical and Materials Transactions B* 14, 325-334.

Ekeroth, E., Roth, O., Jonsson, M., 2006. The relative impact of radiolysis products in radiation induced oxidative dissolution of UO₂. *Journal of Nuclear Materials* 355, 38-46.

Fricke, H., Hart, E.J., 1966. *Chemical dosimetry, Radiation Dosimetry*. Attix F.H. et Roesch W.C, New York, USA.

Grambow, B., Abdelouas, A., Guittonneau, F., Vandenborre, J., Fachinger, J., von Lensa, W., Bros, P., Roudil, D., Perko, J., Marivoet, J., Sneyers, A., Millington, D., Cellier, F., 2008. The Backend of the Fuel Cycle of HTR/VHTR Reactors. *ASME Conference Proceedings*, 649-657.

Grambow, B., Bruno, J., Duro, L., Merino, J., Tamayo, A., Martin, C., Pepin, G., Schumacher, S., Smidt, O., Ferry, C., Jegou, C., Quinoñes, J., Iglesias, E., Rodriguez Villagra, N., Nieto, J.M., Martinez-Esparza, A., Loida, A., Metz, V., Kienzler, B., Bracke, G., Pellegrini, D., Mathieu, G., Wasselin-Trupin, V., Serres, C., Wegen, D., Jonsson, M., Johnson, L., Lemmens, K., Liu, J., Spahiu, K., Ekeroth, E., Casas, I., De Pablo, J., Watson, C., Robinson, P., Hodgkinson, D., 2010. Final Activity Report : Project MICADO Model for Uncertainty for the mechanism of dissolution of spent fuel in nuclear waste repository in: Commission, E. (Ed.), Report.

Hanson, B., McNamara, B., Buck, E., Friese, J., Jenson, E., Krupka, K., Arey, B., 2005. Corrosion of commercial spent nuclear fuel.1. Formation of studtite and metastudtite. *Radiochimica Acta* 93, 159-168.

He, H., Shoesmith, D., 2010. Raman spectroscopic studies of defect structures and phase transition in hyper-stoichiometric UO_{2+x}. *Physical Chemistry Chemical Physics* 12, 8108-8117.

Hoekstra, H.R., Siegel, S., 1973. The uranium trioxide-water system. *Journal of Inorganic and Nuclear Chemistry* 35, 761-779.

Jégou, C., Muzeau, B., Broudic, V., Peugeot, S., Poulesquen, A., Roudil, D., Corbel, C., 2005. Effect of external γ irradiation on dissolution of the spent UO₂ fuel matrix. *Journal of Nuclear Materials* 341, 62-82.

Jonsson, M., Ekeroth, E., Roth, O., 2004. Dissolution of UO₂ by one and two electron oxidants. *Materials Research Society Symposium Proceedings* 807, 77-82.

LaVerne, J.A., Schuler, R.H., 1987. Radiation chemical studies with heavy ions: oxidation of ferrous ion in the Fricke dosimeter. *The Journal of Physical Chemistry* 91, 5770-5776.

Matsui, M., Seki, H., Karasawa, T., Imamura, M., 1970. Radiation Chemical Studies with Cyclotron Beams, (I) Fricke Solution. *Journal of Nuclear Science and Technology* 7, 97-104.

Roth, O., Jonsson, M., 2008. Oxidation of UO₂ (s) in aqueous solution. *Central European Journal of Chemistry* 6, 1-14.

Saini, R.D., Bhattacharyya, P.K., 1987. Radiolytic oxidation of U(IV) sulphate in aqueous solution by alpha particles from cyclotron. *International Journal of Radiation Applications and Instrumentation. Part C. Radiation Physics and Chemistry* 29, 375-379.

Sattonnay, G., Ardois, C., Corbel, C., Lucchini, J.F., Barthe, M.F., Garrido, F., Gosset, D., 2001. α -radiolysis effects on UO₂ alteration in water. *Journal of Nuclear Materials* 288, 11-19.

Sobry, R., 1973. Etude des "uranates" hydrates--II : Examen des proprietes vibrationnelles des uranates hydrates de cations bivalents. *Journal of Inorganic and Nuclear Chemistry* 35, 2753-2768.

Suzuki, T., Abdelouas, A., Grambow, B., Mennecart, T., Blondiaux, G., 2006. Oxidation and dissolution rates of UO₂(s) in carbonate-rich solutions under external α irradiation and initially reducing conditions. *Radiochimica Acta* 94, 567-573.

Titov, M.M., Fachinger, J., Bukaemskiy, A.A., 2004. Investigation of physico-mechanical properties of ceramic oxide kernels for nuclear applications. *Journal of Nuclear Materials* 328, 21-30.

Vandenborre, J., Grambow, B., Abdelouas, A., 2010. Discrepancies in Thorium Oxide Solubility Values: Study of Attachment/Detachment Processes at the Solid/Solution Interface. *Inorganic Chemistry* 49, 8736-8748.

Ziegler, J.F., Biersack, J.P., Littmark, U., 1985. *The Stopping and Range of Ions in Matter*, New York.

Ziegler, J.F., Ziegler, M.D., Biersack, J.P., 2010. SRIM The stopping and range of ions in matter (2010). *Nuclear Instruments and Methods in Physics Research Section B: Beam Interactions with Materials and Atoms* 268, 1818-1823.